Identification and stage-specific association with the translational apparatus of TbZFP3, a CCCH protein that promotes trypanosome life-cycle development

Published in final edited form as:
J Biol Chem. 2006 December 22; 281(51): 39002–39013. doi:10.1074/jbc.M604280200.

Identification and Stage-specific Association with the Translational Apparatus of *Tb*ZFP3, a CCCH Protein That Promotes Trypanosome Life-cycle Development*,s

Athina Paterou[1], **Pegine Walrad**[1], **Paul Craddy**, **Katelyn Fenn**, and **Keith Matthews**[2]
Institute of Immunology and Infection Research, School of Biological Sciences, Ashworth Laboratories, King's Buildings, University of Edinburgh, West Mains Road, Edinburgh EH9 3JT, Scotland, United Kingdom

Abstract

The post-transcriptional control of gene expression is becoming increasingly important in the understanding of regulated events in eukaryotic cells. The parasitic kinetoplastids have a unique reliance on such processes, because their genome is organized into polycistronic transcription units in which adjacent genes are not coordinately regulated. Indeed, the number of RNA-binding proteins predicted to be encoded in the genome of kinetoplastids is unusually large, invoking the presence of unique RNA regulators dedicated to gene expression in these evolutionarily ancient organisms. Here, we report that a small CCCH zinc finger protein, *Tb*ZFP3, enhances development between life-cycle stages in *Trypanosoma brucei*. Moreover, we demonstrate that this protein interacts both with the translational machinery and with other small CCCH proteins previously implicated in trypanosome developmental control. Antibodies to this protein also co-immunoprecipitate EP procyclin mRNA and encode the major surface antigen of insect forms of *T. brucei*. Strikingly, although *Tb*ZFP3 is constitutively expressed, it exhibits developmentally regulated association with polyribosomes, and mutational analysis demonstrates that this association is essential for the expression of phenotype. *Tb*ZFP3 is therefore a novel regulator of developmental events in kinetoplastids that acts at the level of the post-transcriptional control of gene expression.

Regulatory events in prokaryotic and eukaryotic organisms are most commonly governed by transcriptional control. In this way transcription factors and their co-regulators can target the promoters for individual genes or coordinately regulated gene networks enabling either a specific response to an environmental change or a programmed and more widespread response through cell differentiation.

Gene regulation can also operate post-transcriptionally, either at the level of RNA processing, mRNA stability, translational efficiency, protein localization, or turnover (1). The extent of post-transcriptional control of gene expression differs between different genes, networks, cells, and organisms. One group of organisms that has an unusual emphasis on

*This work was supported by the Greek State scholarship foundation and the Wellcome Trust (to A. P.) and by a program grant from the Wellcome Trust (to K. M.).

[S]The on-line version of this article (available at http://www.jbc.org) contains supplemental text and Fig. S1.

[2]To whom correspondence should be addressed. Tel.: 44-131-651-3639; Fax: 44-131-651-3670; E-mail: keith.matthews@ed.ac.uk..
[1]Both authors contributed equally to this work.

Europe PMC Funders Author Manuscripts

post-transcriptional control is the kinetoplastid protozoa, comprising the important human pathogens, *Trypanosoma brucei, Trypanosoma cruzi*, and *Leishmania* sp. (2). These organisms, among the most evolutionarily ancient eukaryotes, are unusual in that their genome is organized into long polycistronic transcription units with tens of genes being coordinately transcribed from distant, as yet unidentified, promoters (3). Such co-transcribed gene clusters do not seem, in general, to be organized as co-regulated operons; instead adjacent genes can show differential gene expression, for example in different life-cycle stages. This places the emphasis of gene regulation in these organisms almost entirely at the post-transcriptional level. However, although the kinetoplastids conserve the conventional eukaryotic machinery for mRNA turnover (4), little is known about the specific trans-acting factors that govern developmental events at the level of gene expression. Moreover, transcriptional control has only been observed for two protein-coding transcription units in *T. brucei*: those encoding the variant surface glycoprotein gene (in bloodstream forms of the parasite) and procyclin genes, which encode a protein coat on the forms of the parasite found in its tsetse fly vector (reviewed in Ref. 2). In contrast to the remainder of trypanosome transcription units these are unique in being transcribed by RNA polymerase I (5, 6).

Differentiation between bloodstream and tsetse-midgut (procyclic) forms of *T. brucei* entails a large number of fundamental changes in these unicellular protozoa (7). In addition to the aforementioned surface antigen exchange, these include changes in cell morphology (8), organelle development and activity (9), metabolism (10, 11), and cell-cycle control (12-14). Usefully, if differentiation is initiated with a subtype of the bloodstream parasite population that accumulates to near homogeneity at the peak of each parasitemia (*i.e.* stumpy forms), then cell differentiation is almost completely synchronous in the population (15). This has allowed a mapping of the events in this developmental pathway, thus revealing a high order of temporal and spatial regulation. It has also allowed the identification of molecules transiently enriched during this process. One such protein, *Tb*ZFP1, has been found to be important for repositioning of the kinetoplast (an elaborated mitochondrial genome) from the posterior end of the cell to a position midway between the nucleus and cell posterior (16, 17). This is one of the major morphological events that characterize differentiation between bloodstream and procyclic forms and is mediated by posterior outgrowth of the trypanosome microtubule corset (8). A related protein, *Tb*ZFP2, also generates a procyclic stage-specific morphological phenotype when overexpressed and is required in bloodstream forms for efficient differentiation, as revealed by transcript-specific RNAi[3] (16).

*Tb*ZFP1 and *Tb*ZFP2 are members of a family of proteins characterized by their possession of the zinc finger motif $C_{7\text{-}8}C_5C_3H$ (CCCH) and small size (<150 amino acids). Although *Tb*ZFP1 and -2 are unique to kinetoplastids, the CCCH motif is an RNA binding zinc finger found in a range of eukaryotic proteins involved at all levels of post-transcriptional gene expression control (18-21). In particular, the mammalian tristetraprolin (TTP) family of proteins recognize AU-rich elements in the 3′-untranslated region of mRNAs causing

[3]The abbreviations used are:

RNAi RNA interference

TTP tristetraprolin

E3 ubiquitin-protein isopeptide ligase

BD binding domain

AD activation domain

regulated instability (18), whereas in *Caenorhabditis elegans* regulated control of translation and mRNA localization during embryonic development is conferred by POS1 (22), MEX3 (23), and PIE-1 (19). Consistent with this, the homologue of *Tb*ZFP1 in *T. cruzi* has been shown to bind RNA and interact with identified regulatory RNA elements that control developmental gene expression (24). Notably, *Tb*ZFP1 and -2 also contain protein-interaction domains with *Tb*ZFP2 possessing a WW motif closely related to one of those found in E3 ubiquitin ligases.

The recent completion of the genome sequence for three kinetoplastids reveals an unusual number of CCCH proteins encoded in each organism, with 65 predicted CCCH proteins encoded in *T. brucei*, compared with 12 in *Schizosaccharomyces pombe* (4). Among this set, a third small CCCH protein has been identified, which enhances trypanosome life-cycle differentiation. Moreover, analysis of the interactions of *Tb*ZFP3 *in vivo* demonstrates its capacity to complex with both *Tb*ZFP1 and *Tb*ZFP2. This supports a modular model for functional interactions among this unusual protein family, each of which has been implicated in the regulation of differentiation events. Finally, we demonstrate that *Tb*ZFP3 exhibits a procyclic stage-specific association with polyribosomes despite its constitutive expression through the life cycle and that this association is necessary for the expression of phenotype. This supports a role for this unique protein family in the post-transcriptional control of developmental events in the trypanosome life cycle.

EXPERIMENTAL PROCEDURES

Trypanosomes

For ectopic expression, *T. brucei* 427 bloodstream and procyclic forms were used, each being previously engineered to express the tetracycline repressor protein, enabling regulated gene expression. Slender and stumpy form RNA, protein extracts, and polysomal extracts were prepared from *T. brucei rhodesiense* EATRO 2340. Stumpy forms were isolated 5-6 days after inoculation of mice with 1×10^5 *T. brucei rhodesiense* EATRO 2340 GUP2962 when the population was >80% stumpy by morphology. Parasite transfection was carried out as previously described (16), with procyclic cells being cultured in SDM-79 and selected with 20 μg/ml hygromycin, whereas bloodstream forms were cultured in HMI-9 (at 37 °C, 5% CO_2) and selected with 2 μg/ml hygromycin.

Plasmid constructs were each generated in the trypanosome expression vector pHD451 (30). Deletion and mutation of *Tb*ZFP3 were carried out either via the Stratagene mutate-a-base mutagenesis kit or by a PCR mutagenesis strategy. Complete details of plasmid constructions in this report, and associated primers, are available from the authors upon request.

Northern and Western Blotting, Immunoprecipitation, and Polysome Fractionation

RNA was prepared from bloodstream or procyclic forms using an RNeasy RNA isolation kit (Qiagen), and RNAs were resolved on 1% formaldehyde gels. Hybridization was carried out using digoxigenin-labeled Riboprobes with post hybridization washes being carried out at 68 °C, 0.1× SSC. Signal detection was via chemiluminescence using CDP-Star (Roche Applied Science) as a reaction substrate.

Protein extracts were prepared from 1×10^6 bloodstream or procyclic forms in Laemmli sample buffer. Samples were transferred to nitrocellulose membranes via electroblotting, and effective transfer was verified by Ponceau staining. Blots were blocked with 5% powdered milk in phosphate-buffered saline overnight and then incubated with 1/500 dilution (in 5% milk in phosphate-buffered saline) of anti-*Tb*ZFP3 antibody, this being raised against the peptide antigen N-DSSQMQQVGHDVPPMA-C in rabbits (by

Eurogentec, Belgium). After incubation with a 1/5000 dilution of anti-rabbit IgG-horseradish peroxidase conjugate (Dako), signals were detected via chemiluminescence.

For immunoprecipitation, 1-5 × 10^8 cells were pelleted and then snap frozen before resuspension in 0.5 ml of IP-150 lysis buffer (10 mM Tris-Cl, pH 8, 150 mM NaCl, 1% Nonidet P-40, 0.5 mM EDTA). After 25-30 strokes in a Dounce homogenizer, the cell extract was cleared by microcentrifugation (10,000 × *g* for 10 min at 4 °C) and used directly for immunoprecipitation, or centrifuged at 100,000 × *g* in a Beckman TLA100.3 rotor to yield a S100 supernatant or pellet. For immunoprecipitation cell extracts were incubated at 4 °C 1 h overnight with antibody (1:500), or with antibody preincubated with the peptide antigen (40 μg) to which it was raised (as a negative control). Washed protein G beads were then incubated with the extract for a further 1 h and pelleted by centrifugation at 10,000 × *g* for 10 min, yielding the flow-through. The beads were washed 6-9 times with IP-150 lysis buffer, and then bound proteins were extracted into boiling Laemmli sample buffer. For RNA immunoprecipitation, the same procedure was used with RNA being isolated in IP-150 lysis buffer plus 1% SDS at 65 °C, and then purified by phenol/chloroform extraction and ethanol precipitation. RNA retrieved from each sample was divided into two reverse transcription reactions using dT_{18}Anchor (GCGCCGGCGCCTCAGCG) primer at 42 °C for 1 h. Equivalent quantities of cDNA obtained from all samples was amplified using the primers 5′-EP1 GGTGCTGCAACGCTGAAATCTGTTGC, or Actin 5′-GTATAGCGTGTGGATTGGCGGTTCC in combination with dT_{18}Anchor at 65 °C for up to 35 cycles.

For polysome fractionation 0.5-1 × 10^9 cells were incubated for 10 min with 100 μg/ml cycloheximide and then centrifuged and resuspended in 25 ml of phosphate-buffered saline containing cycloheximide and washed once. The cells were then resuspended in 1 ml of polysome buffer (20 mM Tris-Cl, pH 7.5, 120 mM KCl, 2 mM $MgCl{\cdot}6H_2O$, 1 mM dithiothreitol, 22 μM leupeptin, with 2 μl of RNasin per milliliter) containing cycloheximide, centrifuged at 1,000 × *g*, resuspended in 0.5 ml of polysome buffer, and subjected to 20 strokes in a Dounce homogenizer with Nonidet P-40 being added to 1.2%. The lysate was cleared by centrifugation at 1,000 × *g*. The lysate was then fractionated on a 15-50% sucrose gradient at 240,000 × *g* in a Beckman SW40Ti rotor, and fractions were collected using a peristaltic pump connected to an AKTA Basic high-performance liquid chromatograph and fraction collector, with RNA concentration being monitored at 254 nm.

Cell Image Acquisition and Morphometric Analysis

Cells were processed for immunofluorescence as previously described. Kinetoplast-posterior measurements were taken using Scion image 1.62. Cell images were captured using a Zeiss Axioscop 2 and processed using Adobe Photoshop CS.

Yeast Two-hybrid Analysis

The Matchmaker system 3 (Clontech) was used throughout, and protocols were followed according to the manufacturer's instructions with the following exceptions: the LexA DNA binding domain plasmid pSTT91 (25) was digested with EcoR1/BamH1to allow for in-frame ligation of the relevant *Tb*ZFP coding region. The activation domain plasmid pGADT7 was created using an EcoR1/XhoI digestion allowing the insertion of the appropriate *Tb*ZFP open reading frame. Co-transformation of 1 μg of both these fusion plasmids into the L40 yeast strain (26) was achieved using the high efficiency polyethylene glycol/lithium acetate method (27), and double transformants were selected on plates lacking Leu and Trp. Activation of the His3 reporter gene by reconstitution of the GAL4 transcription factor encoded in the fusion proteins was characterized by growth on plates lacking Leu/Trp/His/Ade. Activation of the β-galactosidase reporter gene was observed by

replica-plating the colonies onto nylon membrane (Amersham Biosciences) on a YPDa plate, incubating for 16 h, and then performing a colony lift assay (28).

RESULTS

We searched the *T. brucei* genome sequence data base (www.geneDB.org) using the *Tb*ZFP1 and *Tb*ZFP2 protein sequences to identify further members of this protein family. This identified an open reading frame (Tb927.3.720) encoding a 130-amino acid predicted protein comprising a CCCH domain toward its C terminus and a WW protein-interaction domain toward its N terminus (Fig. 1*A*). This matched the overall motif organization of *Tb*ZFP2 (Tb11.01.6590), which has been previously characterized to have a role in trypanosome differentiation and posterior end morphogenesis (16). Similar to *Tb*ZFP2, the WW domain in the newly identified protein was most similar to a particular WW domain in E3 ubiquitin ligases. Unlike *Tb*ZFP2, however, *Tb*ZFP3 also possessed three intact copies of the RGG-predicted RNA-binding motif positioned centrally between the WW and CCCH domain. The newly identified gene has been recently described in the context of a bioinformatic analysis of homologous genes in *T. cruzi* and has been named *Tc*ZFP2b (29). However, although they share several motifs associated with molecular interactions, the primary amino acid sequences of *Tb*ZFP2a and -b are dissimilar (Fig. 1*A*), and their genes are unlinked. Therefore, we prefer to denote this by renaming of the new molecule *Tb*ZFP3.

The previously characterized differentiation regulator *Tb*ZFP1 is silenced in bloodstream forms at the protein level but is transiently elevated during differentiation to procyclic forms where expression is then retained (16, 17). In contrast, *Tb*ZFP2 is expressed equally in bloodstream and procyclic forms and exhibits uniform expression throughout synchronous differentiation between stumpy and procyclic forms (16). To address whether *Tb*ZFP3 is regulated during the parasite life cycle, we examined the mRNA and protein levels for this gene in bloodstream and procyclic forms. Fig. 1*B* demonstrates that this 390-bp-coding region is contained within an mRNA of ~1.9 kb that is expressed equally in slender and stumpy bloodstream forms and in procyclic forms. To verify that the gene was translated into protein and to examine its expression profile, an anti-peptide antibody was raised to the sequence N-DSSQMQQVGHDVPPMA-C, this being located at the extreme C terminus of *Tb*ZFP3 protein. When reacted with protein derived from bloodstream monomorphic forms and procyclic forms, a band was detected at the predicted molecular mass for *Tb*ZFP3 (14 kDa) in each life-cycle stage, and at approximately equal levels, consistent with the RNA profile (Fig. 1*B*). The profile of *Tb*ZFP3 protein expression was also assayed during synchronous differentiation between bloodstream stumpy forms and procyclic forms, after culture in SDM-79 medium at 27 °C containing 6 m_M *cis*-aconitate (Fig. 1*C*). This demonstrated approximately equivalent expression throughout differentiation with no evidence for a transient elevation in expression during this synchronous transition. This matched the expression profile of *Tb*ZFP2 but differs from *Tb*ZFP1, which is elevated in expression level around 4-8 h through differentiation (16). Therefore, *Tb*ZFP3 is consistently expressed in both bloodstream and procyclic forms and during synchronous differentiation between these forms.

Ectopic Expression of TbZFP3 Induces Enhanced Differentiation

Prior knockdown of *Tb*ZFP2 in bloodstream forms by RNAi had resulted in decreased efficiency of differentiation as assessed by gain of the insect-stage-specific antigen, EP procyclin (16). This implicated *Tb*ZFP2 in the control of early differentiation events, contrasting with *Tb*ZFP1, which appears to act later in the differentiation program (17). To determine whether *Tb*ZFP3 also had a role in developmental control, we initially attempted RNAi for this molecule in bloodstream forms. Although viable cell lines were generated using several available RNAi vectors, effective reduction of *Tb*ZFP3 protein was not

achieved (a maximum reduction of 60% was observed, data not shown). However, cell lines were generated in which tetracycline-regulated ectopic overexpression of *Tb*ZFP3 was possible. Specifically, a copy of *Tb*ZFP3 encoding a C-terminal Ty1 epitope tag (denoted *Tb*ZFP3-Ty) was inserted into the trypanosome expression vector pHD451 (30) and transfected into *T. brucei* 427 monomorphic bloodstream forms, which express the tetracycline repressor protein. The resulting cell lines were then induced to express *Tb*ZFP3-Ty by the addition of tetracycline, this being monitored by Western blotting using the *Tb*ZFP3-specific anti-peptide antibody allowing simultaneous detection of the endogenous and transgenic protein. Fig. 2*B* (*Day 0* samples) shows inducible ectopic expression of *Tb*ZFP3-Ty in bloodstream forms was achieved, generating a combined 1- to 2-fold overexpression of *Tb*ZFP3 compared with wild-type cells.

Having successfully generated a cell line capable of perturbed *Tb*ZFP3 expression we examined the consequences of this for the efficiency of differentiation to procyclic forms. Specifically, parental or *Tb*ZFP3-Ty-transfected bloodstream forms were induced, or not, with tetracycline for 3 days in culture, and then differentiation was initiated under standard conditions. Thereafter, EP procyclin expression was followed daily via immunofluorescence, with protein samples also being prepared to monitor *Tb*ZFP3-Ty expression. Fig. 2*A* (*days 1-3* samples) shows the result of four such experiments, which revealed that ectopic expression of *Tb*ZFP3-Ty resulted in enhanced EP procyclin expression in the population. Thus, at each time point after the induction of differentiation the proportion of EP procyclin expressers was consistently up to 2-fold higher than in uninduced or parental controls (either in the presence or absence of tetracycline). This correlated with the detection of the ectopically expressed protein by Western blotting (Fig. 2*B*). To complement this IFA-based counting assay (which qualitatively scores cells as being "+" or "-" on an individual cell basis), differentiation was also scored in an independent experiment by flow cytometry for EP expression at the population level (Fig. 2*C*). This confirmed enhanced differentiation upon *Tb*ZFP3-Ty expression with the induced cell line demonstrating 69% EP-procyclin expression compared with 53% in the uninduced control at 72 h after the initiation of differentiation. We verified that this effect was not due to the increased expression of stumpy characteristics via a number of assays for that life-cycle stage and found no consistent difference from uninduced cells (refer to the supplemental data). Therefore, ectopic expression of *Tb*ZFP3 results in enhanced differentiation to procyclic forms as assessed by EP procyclin expression, consistent with the reduced efficiency of this process upon knockdown of *Tb*ZFP2 by RNAi (16). Combined with the specific inhibition of kinetoplast repositioning induced by genetic ablation of *Tb*ZFP1 (17), this supports the role for this family of proteins in differentiation processes.

Ectopic Expression in Procyclic Forms Causes a Characteristic Morphological Phenotype

In addition to the bloodstream form cell lines, ectopic expression of *Tb*ZFP3 was also investigated in procyclic forms (Fig. 3*A*). In this case, upon induction of *Tb*ZFP3-Ty expression, the cell population was found to produce elongated cells reminiscent of the nozzle phenotype previously observed upon ectopic expression of *Tb*ZFP2 (16) (Fig. 3*B*). As with *Tb*ZFP2 expression, cell elongation upon *Tb*ZFP3 expression involved posterior microtubule extension as revealed by YL1/2 staining of tyrosinated α-tubulin in the trypanosome cytoskeleton (data not shown). However, unlike with ectopic *Tb*ZFP2 expression, where nozzle formation was entirely restricted to cells with 1 kinetoplast and 1 nucleus (*i.e.* G_1 and S phase cells), in cells expressing ectopic *Tb*ZFP3-Ty ~15% of cells with an extended posterior had segregated their kinetoplast. This is indicative of cell cycle progression into G_2, consistent with a similar phenotype observed upon RNAi ablation of the cyclin, CYC2 (31).

The manifestation of the nozzle morphology provided a convenient and quantifiable phenotypic assay with which to dissect important domains in *Tb*ZFP3. Specifically we wanted to evaluate whether the WW domain and CCCH RNA binding domain in *Tb*ZFP3 were essential for morphological extension. Therefore, we generated a series of cell lines in which either the WW or CCCH domain in *Tb*ZFP3 were deleted from the ectopically expressed protein, or in which a single amino acid change was introduced to mutate the CCCH motif to the sequence CCAH. Finally, we generated a cell line in which the Ty tag was absent from the transgenic protein thereby ensuring that phenotypic effects were a result of the native protein and not the introduction of the tag. Fig. 4*A* shows that in each case the ectopic proteins were effectively expressed in the transgenic cell lines. The relative expression between induced and uninduced samples varied somewhat, but in each the level of the induced protein expression was similar. Having verified effective and comparable expression levels for each protein, we then assayed the degree of morphological extension by measuring the kinetoplast to posterior dimension in 100 cells in each population. This analysis, shown in Fig. 4*B*, demonstrated that, whereas the presence or absence of the Ty tag was not important in nozzle formation, deletion of the WW or CCCH domain, or introduction of a mutation to disrupt the CCCH domain, each significantly abrogated nozzle formation. Thus ectopic expression of either native or Ty-tagged *Tb*ZFP3 generated a mean kinetoplast-posterior dimension of 10.31 μm (±0.35 μm (S.E.)) and 9.52 μm (±0.24 μm) respectively, whereas the values generated for each mutant were: ΔWW, 5.24 μm (±0.21 μm), ΔCCCH 5.40 μm (±0.21 μm), and CCAH, 5.88 μm (±0.19 μm), with these approximating to the kinetoplast-posterior dimension in wild-type procyclic forms of 5.41 μm (±0.18 μm). We conclude that the CCCH and WW domains in *Tb*ZFP3 are both individually important for generation of the nozzle phenotype.

Molecular Interactions of the TbZFP Protein Family

We have proposed that members of the *Tb*ZFP family may interact on the basis of complementary protein interaction domains whereby *Tb*ZFP2 and -3 each contain a WW domain, and *Tb*ZFP1 contains the complementary target PPPPPY motif (16). To investigate this potential, the ability of *Tb*ZFP1, *Tb*ZFP2, and *Tb*ZFP3 to interact in a pairwise yeast two-hybrid interaction screen was assayed. Thus fusion proteins of *Tb*ZFP1, *Tb*ZFP2, and *Tb*ZFP3 were generated in bait and prey plasmids, which allowed expression of each *Tb*ZFP fused to either the LEXA DNA binding domain (BD) or the GAL4 activation domain (AD). In each case mutants, in which the WW domain in both *Tb*ZFP2 and -3 were deleted, were also generated to establish their function in potential interactions with *Tb*ZFP1. These molecules were then co-transformed pairwise into yeast and colonies streaked onto nonselective (-*TRP* and -*LEU*) or selective (-*ADE* and -*HIS*) plates, as well as being assayed for LacZ production.

The data in Fig. 5 indicate that *Tb*ZFP1 is able to directly interact with *Tb*ZFP2 and -3, this evidenced by the production of LacZ and activation of nutritional markers on -*TRP*, -*LEU*, -*HIS*, and -*ADE* plates (*2DB*+*1AD* and *3DB*+*1AD*, Fig. 5). Moreover, this interaction is mediated by the WW motif alone, because deletion of this motif in *Tb*ZFP2 (*2DB*Δ*ww* +*1AD*, Fig. 5) or *Tb*ZFP3 (*3DB*Δ*ww*+*1AD*, Fig. 5) abolishes the interaction of each with *Tb*ZFP1. Although a weak potential interaction was observed between the *Tb*ZFP2-LexA DNA BD fusion and the *Tb*ZFP3-Gal4AD fusion (*2DB*+*3AD*, Fig. 5), this was not reciprocated when the bait and prey were reversed and is likely to be artifactual. Thus, there appears to be no direct interaction between *Tb*ZFP2 and *Tb*ZFP3 and we found no evidence that these proteins can homodimerize. However, *Tb*ZFP1 can interact with *Tb*ZFP2 or *Tb*ZFP3 with the WW protein binding motifs being essential in this.

Although two-hybrid analysis can prove informative for direct protein interactions *in vitro*, it was also important to validate potential interactions between these proteins *in vivo*.

Therefore, the ability of the antibody against *Tb*ZFP3 to co-immunoprecipitate *Tb*ZFP2 and *Tb*ZFP1 was investigated in procyclic cell extracts, with specificity being verified by blocking with the peptide antigen used to raise the antibody. Fig. 6*A* demonstrates that *Tb*ZFP1, -2, and -3 were each co-immunoprecipitated with anti-*Tb*ZFP3 antibody and that this was efficiently blocked by the peptide immunogen. These experiments confirm that *Tb*ZFP1 can interact directly with *Tb*ZFP2 and *Tb*ZFP3 *in vitro* and that all three proteins can be co-immunoprecipitated *in vivo* suggesting their involvement in overlapping or the same protein complex(es).

Cell Fractionation of TbZFP3 Reveals Stage-specific Association with Polyribosomes

To analyze further the cellular location and interactions of *Tb*ZFP3, the distribution of this protein among different cellular compartments was investigated by cell lysis and differential detergent extraction. This resolved trypanosome proteins into cytosolic, nuclear, organellar vesicles/plasma membrane, or cytoskeletal fractions. Fig. 6*B* demonstrates that the majority of *Tb*ZFP3 co-fractionated with cytosolic proteins in both bloodstream and procyclic forms, with a small proportion fractionating with cell organelles/plasma membrane, this most probably representing some cytosolic contamination of this fraction. This distribution was matched by *Tb*ZFP2. Consistent with a cytosolic location, immunofluorescence of *Tb*ZFP3 in procyclic forms (fixed by paraformaldehyde in the presence of 0.1% Triton X-100) revealed a uniform staining pattern through the cell, without concentration in any recognizable organelle (data not shown).

Cell extracts were also analyzed by differential centrifugation, revealing a distribution of *Tb*ZFP3 between S100 supernatant and pellet (data not shown). This suggested the possibility of association of *Tb*ZFP3 with polysomes in procyclic forms. To investigate this further, procyclic cell extracts prepared in polysome buffer in the presence of cycloheximide were separated on 15-50% sucrose gradients, and fractions were analyzed for the presence of *Tb*ZFP3, BiP (a non-polysomal endoplasmic reticulum protein) and ribosomal protein P0 (a ribosomal stalk component that fractionates with monosomes and polysomes). Fig. 7 shows that *Tb*ZFP3 distributed into monosomal (fractions 6-12) and polysomal fractions (fractions 13-22) matching the distribution of P0, although *Tb*ZFP3 was also abundant in the non-polysomal fractions, consistent with the bimodal distribution of *Tb*ZFP3 between the S100 pellet and supernatant. Confirming the association of *Tb*ZFP3 with polysomes in procyclic forms, *Tb*ZFP3 and P0 redistributed to lower molecular weight fractions in EDTA-treated cell extracts (Fig. 7).

The stage-specific phenotypes resulting from *Tb*ZFP3 ectopic expression prompted us to investigate the polysome association of this protein in bloodstream forms, as well as procyclic forms. Interestingly, although *Tb*ZFP3 is expressed at similar levels in bloodstream and procyclic forms, clear evidence for polysome association was only observed in the latter (Fig. 8*A*). Thus, in bloodstream slender forms, *Tb*ZFP3 sedimented in the low molecular weight fractions with a distinct distribution from the polysomal marker P0. Similarly, in homogenous populations of bloodstream stumpy forms *Tb*ZFP3 was also disassociated from polyribosomes, although the abundance of polysomes was considerably reduced as expected in this quiescent life-cycle stage (32). This demonstrated that the association of *Tb*ZFP3 with polysomal fractions was developmentally regulated, being enriched in procyclic forms and absent in bloodstream slender and stumpy forms.

The stage-specific association of *Tb*ZFP3 with polyribosomes prompted us to further determine whether ectopic expression of this protein perturbed its normal associations with the translational apparatus in either bloodstream or procyclic forms. Thus, we examined the distribution of endogenous and ectopic *Tb*ZFP3 in either transgenic procyclic forms (where the nozzle phenotype is generated) or in bloodstream forms (which exhibit enhanced

differentiation). More specifically, *Tb*ZFP3 was expressed in either procyclic forms for 48 h (coinciding with the appearance of nozzle cells in the population) or in a bloodstream line that can generate division-arrested intermediate/stumpy forms when grown in mice (33). These cells were grown for 8 days in mice that had been supplied with doxycycline in their drinking water (to induce *Tb*ZFP3-Ty expression), and then parasites were harvested for analysis of the distribution of *Tb*ZFP3 on sucrose gradients. Fig. 8*B* demonstrates that in both bloodstream and procyclic forms the ectopically expressed and endogenous *Tb*ZFP3 exactly co-sedimented, this being polysomal for procyclic forms and non-polysomal for the bloodstream forms. We conclude that ectopically expressed *Tb*ZFP3 does not alter the normal polysomal distribution of this protein, association of the translational apparatus being enriched in procyclic forms regardless of the expression of ectopic *Tb*ZFP3.

Polysome Association Precisely Correlates with Both Nozzle Formation and Enhanced Differentiation

In procyclic forms the morphological phenotype generated by *Tb*ZFP3 ectopic expression was dependent upon the integrity of the WW and CCCH domain. To investigate whether disruption of these domains resulted in disassociation of the ectopic protein from polysomes, the distribution of endogenous and ectopically expressed *Tb*ZFP3 was analyzed on sucrose gradients of procyclic cell extracts. In each case the ectopic and endogenous proteins were detected using either the anti-Ty1 epitope tag antibody BB2 (to detect the ectopic protein only) or the *Tb*ZFP3 antibody (detecting both endogenous and ectopic *Tb*ZFP3). Fig. 9 demonstrates that, when the ΔWW, ΔCCCH, or CCAH mutants were expressed in procyclic forms, the ectopic protein fractionated into the non-polysomal or monosomal region of the gradient, whereas endogenous *Tb*ZFP3 and the ribosomal marker P0 each remained polysome-associated. This demonstrates that *Tb*ZFP3 associates with polysomes only if its WW or CCCH domains are intact. This exactly correlates with the capacity of each mutant to induce morphological extension as determined in Fig. 4.

Having determined that mutations that prevented polysome association also prevented nozzle formation in procyclic forms, we investigated whether the same mutants also disrupted enhanced differentiation of bloodstream forms. Therefore, stable bloodstream trypanosome cell lines were generated expressing each of the *Tb*ZFP3 mutants (ΔWW, ΔCCCH, and CCAH), and the expression of these was induced for 3 days by growth in tetracycline. Thereafter, each was induced to initiate differentiation with *cis*-aconitate, and the percentage of procyclin expressers quantified over the following 72 h by immunofluorescence. Fig. 10 shows that, whereas ectopic expression of wild-type *Tb*ZFP3 enhanced differentiation as expected, the mutants with a disrupted WW or CCCH domain each differentiated with an equivalent efficiency to wild-type parental cells. This demonstrated that the phenotypes generated by ectopic expression of *Tb*ZFP3 in both procyclic forms (nozzle formation) and bloodstream forms (enhanced differentiation) were each dependent upon the integrity of the WW and CCCH domain in the protein. Moreover, manifestation of these phenotypes exactly correlated with the ability of each protein to associate with polysomes. This provides evidence for a cause-and-effect relationship between the function of *Tb*ZFP3 and its association with the translational apparatus.

The enhanced differentiation phenotype induced by TbZFP3 ectopic expression was detected by assay for the expression of EP procyclin protein. Therefore, we assessed whether antibodies to TbZFP3 could co-immunoprecipitate EP procyclin mRNA. Fig. 11*A* demonstrates that this was the case: EP procyclin mRNA was selected by antibody to TbZFP3 (Fig. 11*A*, *lane 1*), and this was prevented in the presence of blocking peptide (Fig. 11*A*, *lane 2*). The specificity of this was confirmed by the absence of actin mRNA, a constitutively expressed transcript, in the immunoprecipitated material (Fig. 11*B*). We

conclude that TbZFP3 protein and EP procyclin mRNA co-precipitate in procyclic cells, either directly or indirectly.

DISCUSSION

The control of cell differentiation in *T. brucei* is highly regulated, involving a series of developmental steps that are temporally coordinated. This ensures the generation of a viable cell upon differentiation from the bloodstream to the very different environment of the tsetse midgut. The control of these cellular events requires changes in gene expression, this effected by unknown regulatory factors that must operate at the post-transcriptional level. In this report we demonstrate that a new member of a previously characterized family of unusual small RNA-binding proteins is able to enhance differentiation when overexpressed. Moreover, we demonstrate that *Tb*ZFP3 exhibits developmentally regulated co-fractionation with polyribosomes. To our knowledge this is the first regulatory protein identified in these organisms that controls differentiation capacity and shows life-cycle stage-specific phenotypes via involvement at a specific step in the gene expression pathway, the translational apparatus.

*Tb*ZFP3 was identified on the basis of its possession of a CCCH zinc finger domain. This motif is characterized by its interaction with RNA in a number of regulatory proteins in eukaryotic cells, including trypanosomes (24). The best characterized of these is the TTP family of mRNA regulators, which destabilize specific cytokine transcripts important in regulating immune responses. In TTP knock-out mice, dysregulation of tumor necrosis factor-α and granulocyte macrophage-colony stimulating factor in macrophages is observed as are changes in the abundance of at least two interleukin transcripts (reviewed in Ref. 34). These changes are caused by binding of TTP to AU-rich elements in the 3′-untranslated region of target mRNAs, resulting in their destabilization. In addition to TTP family proteins, a number of different classes of CCCH-containing molecule with a diversity of functions have subsequently been characterized in eukaryotic cells. These include the regulation of flower development by HUA1 (35) and FES1 (36), proteins that protect against viral infection by destabilization of retroposon transcripts (37), components of the mRNA processing machinery (U2AF, CPSF30, suppressor of sable), and a number of developmental regulators in *C. elegans*, which function via temporal and spatial regulation of maternal mRNAs at several levels (transcription, mRNA processing, RNA localization, and translation) (19, 38, 39).

The binding of CCCH-containing proteins to RNA is normally dependent upon the presence of two tandemly arranged CCCH zinc finger motifs (40, 41), these being at precisely conserved spacing. In contrast to this organization, *Tb*ZFP3, like the previously identified *Tb*ZFP1 and *Tb*ZFP2, possesses only a single CCCH domain. Although one CCCH domain is sufficient for RNA binding *in vitro* (27),[4] we investigated whether *Tb*ZFP1, -2, or -3 could interact to generate a multicomponent complex (possibly an mRNP complex) possessing more than one CCCH finger. Initially, yeast two-hybrid studies confirmed the ability of *Tb*ZFP2 and -3 to interact with *Tb*ZFP1, this being mediated via the WW domain in each protein. This matches the findings of a related study with an analogous protein identified in *T. cruzi* (29), although in contrast to that study we did not find evidence that *Tb*ZFP2 or *Tb*ZFP3 could homodimerize. More importantly, when we investigated the association of *Tb*ZFP3 with *Tb*ZFP1 and *Tb*ZFP2 *in vivo* via co-immunoprecipitation we found evidence for direct or indirect interaction between each protein, providing evidence that these proteins can co-associate in the cell.

[4]P. Walrad and K. Matthews, unpublished observations.

Analysis of the polysomal distribution of *Tb*ZFP3 revealed that this protein (and *Tb*ZFP2)[4] showed stage-enriched association with the translational apparatus. Based on this surprising observation, we propose that *Tb*ZFP3 operates as a trans-acting regulator to translationally activate (or repress, if the protein acts on a negative regulator) specific mRNA subsets in a developmentally regulated manner. This scenario is compatible with the phenotypes observed in both procyclic and bloodstream forms when *Tb*ZFP3 is ectopically overexpressed. Thus, in procyclic forms, posterior extension to generate nozzle forms represents an exaggerated manifestation of the normal morphological changes that occur during differentiation. In bloodstream forms, *Tb*ZFP3 ectopic expression would have no consequence until differentiation was initiated, and the protein associates with the translational apparatus. As in established procyclic forms, this would then result in the robust expression of procyclic characteristics (*e.g.* procyclin expression and kinetoplast positioning), this being manifested as more efficient differentiation. Therefore, direct or indirect regulation of differentiation markers such as EP procyclin is possible, and indeed we found that TbZFP3 is able to co-immunoprecipitate EP procyclin transcripts. This does not indicate direct binding, although *Tc*ZFP1 from *T. cruzi* (related to *Tb*ZFP1 in *T. brucei*) can directly interact with a procyclin regulatory element *in vitro* (24). Consistent with the association of *Tb*ZFP3 with polysomes only after the initiation of differentiation to procyclic forms, we observed no pre-expression of mRNA or protein for EP procyclin or the procyclic-specific cytoskeletal protein CAP 5.5 upon *Tb*ZFP3 ectopic expression in bloodstream forms.[5]

Several RNA-binding proteins regulate developmental pathways via translational control. Examples include the *Drosophila* Bruno protein that interacts with the Oskar embryonic mRNA and silences its translation via sequestration into silencing particles (42). Similarly, in *C. elegans* the CCCH protein POS-1 controls embryonic development via translational regulation of the maternal mRNA glp-1 (39). In another case, PIE-1 regulates the association of mRNAs with stress granules, such that they are repressed (38). The paucity of transcriptional control, and the polycistronic organization of the genome, make post-transcriptional mechanisms the most important level for gene regulation in trypanosomes. To date, most attention has focused on the role of differential mRNA stability for stage-regulated transcripts. However, it is increasingly clear that translational control is also a major component of regulated gene expression in trypanosomatids. This matches the emerging picture for genes in other organisms in which developmental processes are controlled via pre-existing mRNAs being held in a translationally inactive state (34, 43) often by sequestration into ribonuclear granules (P bodies).

*Tb*ZFP3, like *Tb*ZFP2, is constitutively expressed. However, its association with other RNA-binding proteins may modify its activity or substrate specificity. One of these modulators may be *Tb*ZFP1. *Tb*ZFP1 is synthesized only after the initiation of differentiation between bloodstream and procyclic forms such that association with *Tb*ZFP2, or *Tb*ZFP3 (or a complex containing both proteins), may alter their target specificity. This proposed modularization of function may allow these proteins to control the expression of distinct cohorts of genes in different life-cycle stages, or at stages through development, in a form of post-transcriptional operonic regulation (44). A general perturbation of protein translation induced by *Tb*ZFP3 expression is ruled out by the observation that P0 does not redistribute into monosomes upon ectopic *Tb*ZFP3 expression. Furthermore, general translational inhibition in procyclic forms by hygromycin does not induce comparable nozzle formation.[5]

[5]A. Paterou, P. Walrad, P. Craddy, K. Fenn, and K. Matthews, unpublished observations.

Europe PMC Funders Author Manuscripts

The *Tb*ZFP family of RNA-binding proteins are present in kinetoplastid parasites but not in other eukaryotes for which there is complete genome sequence information. Indeed, in kinetoplastids there is over five times the number of CCCH proteins as in yeast. It is likely that the unique reliance upon post-transcriptional control by the trypanosome genome necessitates this plethora of novel RNA-binding proteins, which permit stringent and rapid control of gene expression during the parasite life cycle. Although many of the core components of the gene expression machinery in these parasites are conserved with their hosts and vectors, it is those components that are not present in other organisms that provide the key to understanding the unique complexity of gene regulation in these organisms. The *Tb*ZFP family of CCCH proteins provides an excellent route into dissecting the molecular interactions required for coordinating a developmental pathway almost completely dependent on the post-transcriptional control of gene expression.

Supplementary Material

Refer to Web version on PubMed Central for supplementary material.

Acknowledgments

We thank Jay Bangs and Steven Reed for the gifts of antibodies to BiP and T. cruzi P0, respectively. The L40 and AMR70 yeast strains and pSTT91 yeast vector were provided courtesy of R. Sternglanz, Center for Yeast Genetics, Stony Brook University, New York, NY.

REFERENCES

1. Moore MJ. Science. 2005; 309:1514–1518. [PubMed: 16141059]
2. Clayton CE. EMBO J. 2002; 21:1881–1888. [PubMed: 11953307]
3. Berriman M, Ghedin E, Hertz-Fowler C, Blandin G, Renauld H, Bartholomeu DC, Lennard NJ, Caler E, Hamlin NE, Haas B, Bohme U, Hannick L, Aslett MA, Shallom J, Marcello L, Hou L, Wickstead B, Alsmark UC, Arrowsmith C, Atkin RJ, Barron AJ, Bringaud F, Brooks K, Carrington M, Cherevach I, Chillingworth TJ, Churcher C, Clark LN, Corton CH, Cronin A, Davies RM, Doggett J, Djikeng A, Feldblyum T, Field MC, Fraser A, Goodhead I, Hance Z, Harper D, Harris BR, Hauser H, Hostetler J, Ivens A, Jagels K, Johnson D, Johnson J, Jones K, Kerhornou AX, Koo H, Larke N, Landfear S, Larkin C, Leech V, Line A, Lord A, Macleod A, Mooney PJ, Moule S, Martin DM, Morgan GW, Mungall K, Norbertczak H, Ormond D, Pai G, Peacock CS, Peterson J, Quail MA, Rabbinowitsch E, Rajandream MA, Reitter C, Salzberg SL, Sanders M, Schobel S, Sharp S, Simmonds M, Simpson AJ, Tallon L, Turner CM, Tait A, Tivey AR, Van Aken S, Walker D, Wanless D, Wang S, White B, White O, Whitehead S, Woodward J, Wortman J, Adams MD, Embley TM, Gull K, Ullu E, Barry JD, Fairlamb AH, Opperdoes F, Barrell BG, Donelson JE, Hall N, Fraser CM, Melville SE, El-Sayed NM. Science. 2005; 309:416–422. [PubMed: 16020726]
4. Ivens AC, Peacock CS, Worthey EA, Murphy L, Aggarwal G, Berriman M, Sisk E, Rajandream MA, Adlem E, Aert R, Anupama A, Apostolou Z, Attipoe P, Bason N, Bauser C, Beck A, Beverley SM, Bianchettin G, Borzym K, Bothe G, Bruschi CV, Collins M, Cadag E, Ciarloni L, Clayton C, Coulson RM, Cronin A, Cruz AK, Davies RM, De Gaudenzi J, Dobson DE, Duesterhoeft A, Fazelina G, Fosker N, Frasch AC, Fraser A, Fuchs M, Gabel C, Goble A, Goffeau A, Harris D, Hertz-Fowler C, Hilbert H, Horn D, Huang Y, Klages S, Knights A, Kube M, Larke N, Litvin L, Lord A, Louie T, Marra M, Masuy D, Matthews K, Michaeli S, Mottram JC, Muller-Auer S, Munden H, Nelson S, Norbertczak H, Oliver K, O'neil S, Pentony M, Pohl TM, Price C, Purnelle B, Quail MA, Rabbinowitsch E, Reinhardt R, Rieger M, Rinta J, Robben J, Robertson L, Ruiz JC, Rutter S, Saunders D, Schafer M, Schein J, Schwartz DC, Seeger K, Seyler A, Sharp S, Shin H, Sivam D, Squares R, Squares S, Tosato V, Vogt C, Volckaert G, Wambutt R, Warren T, Wedler H, Woodward J, Zhou S, Zimmermann W, Smith DF, Blackwell JM, Stuart KD, Barrell B, Myler PJ. Science. 2005; 309:436–442. [PubMed: 16020728]
5. Rudenko G, Bishop D, Gottesdiener K, Van der Ploeg LHT. EMBO J. 1989; 8:4259–4263. [PubMed: 2591373]

6. Gunzl A, Bruderer T, Laufer G, Schimanski B, Tu LC, Lee PI, Lee MG. Eukaryot. Cell. 2003; 2:542–551. [PubMed: 12796299]
7. Matthews KR. J. Cell Sci. 2005; 118:283–290. [PubMed: 15654017]
8. Matthews KR, Sherwin T, Gull K. J. Cell Sci. 1995; 108:2231–2239. [PubMed: 7673343]
9. Priest JW, Hajduk SL. J. Bioenerg. Biomembr. 1994; 26:179–191. [PubMed: 8056785]
10. Tielens AGM, VanHellemond JJ. Parasitol. Today. 1998; 14:265–271. [PubMed: 17040781]
11. van Weelden SW, Fast B, Vogt A, van der Meer P, Saas J, van Hellemond JJ, Tielens AG. J. Biol. Chem. 2003; 278:12854–12863. [PubMed: 12562769]
12. Hammarton TC, Clark J, Douglas F, Boshart M, Mottram JC. J. Biol. Chem. 2003; 278:22877–22886. [PubMed: 12682070]
13. Tu X, Mancuso J, Cande WZ, Wang CC. J. Cell Sci. 2005; 118:4353–4364. [PubMed: 16144864]
14. Tu X, Wang CC. Mol. Biol. Cell. 2005; 16:97–105. [PubMed: 15525678]
15. Ziegelbauer K, Quinten M, Schwarz H, Pearson TW, Overath P. Eur. J. Biochem. 1990; 192:373–378. [PubMed: 1698624]
16. Hendriks EF, Robinson DR, Hinkins M, Matthews KR. EMBO J. 2001; 20:6700–6711. [PubMed: 11726506]
17. Hendriks EF, Matthews KR. Mol. Microbiol. 2005; 57:706–716. [PubMed: 16045615]
18. Blackshear PJ. Biochem. Soc. Trans. 2002; 30:945–952. [PubMed: 12440952]
19. Reese KJ, Dunn MA, Waddle JA, Seydoux G. Mol. Cell. 2000; 6:445–455. [PubMed: 10983990]
20. Tacahashi Y, Helmling S, Moore CL. Nucleic Acids Res. 2003; 31:1744–1752. [PubMed: 12626716]
21. Wentz-Hunter K, Potashkin J. Nucleic Acids Symp. Ser. 1995; 33:226–228. [PubMed: 8643378]
22. Tabara H, Hill RJ, Mello CC, Priess JR, Kohara Y. Development. 1999; 126:1–11. [PubMed: 9834181]
23. Guedes S, Priess J. Development. 1997; 124:731–739. [PubMed: 9043088]
24. Morking PA, Dallagiovanna BM, Foti L, Garat B, Picchi GF, Umaki AC, Probst CM, Krieger MA, Goldenberg S, Fragoso SP. Biochem. Biophys. Res. Commun. 2004; 319:169–177. [PubMed: 15158457]
25. Sutton A, Heller RC, Landry J, Choy JS, Sirko A, Sternglanz R. Mol. Cell Biol. 2001; 21:3514–3522. [PubMed: 11313477]
26. Hollenberg SM, Sternglanz R, Cheng PF, Weintraub H. Mol. Cell Biol. 1995; 15:3813–3822. [PubMed: 7791788]
27. Gietz D, St Jean A, Woods RA, Schiestl RH. Nucleic Acids Res. 1992; 20:1425. [PubMed: 1561104]
28. Breeden L, Nasmyth K. Cold Spring Harbor Symp. Quant. Biol. 1985; 50:643–650. [PubMed: 3938367]
29. Caro F, Bercovich N, Atorrasagasti C, Levin MJ, Vazquez MP. Biochem. Biophys. Res. Commun. 2005; 333:1017–1025. [PubMed: 15964555]
30. Biebinger S, Wirtz LE, Lorenz P, Clayton C. Mol. Biochem. Parasitol. 1997; 85:99–112. [PubMed: 9108552]
31. Hammarton TC, Engstler M, Mottram JC. J. Biol. Chem. 2004; 279:24757–24764. [PubMed: 15039435]
32. Brecht M, Parsons M. Mol. Biochem. Parasitol. 1998; 97:189–198. [PubMed: 9879897]
33. van Deursen FJ, Shahi SK, Turner CM, Hartmann C, Guerra-Giraldez C, Matthews KR, Clayton CE. Mol. Biochem. Parasitol. 2001; 112:163–171. [PubMed: 11223123]
34. Barreau C, Paillard L, Osborne HB. Nucleic Acids Res. 2005; 33:7138–7150. [PubMed: 16391004]
35. Chen X, Meyerowitz EM. Mol. Cell. 1999; 3:349–360. [PubMed: 10198637]
36. Schmitz RJ, Hong L, Michaels S, Amasino RM. Development. 2005; 132:5471–5478. [PubMed: 16291783]
37. Gao G, Guo X, Goff SP. Science. 2002; 297:1703–1706. [PubMed: 12215647]

38. Tenenhaus C, Subramaniam K, Dunn MA, Seydoux G. Genes Dev. 2001; 15:1031–1040. [PubMed: 11316796]
39. Ogura K, Kishimoto N, Mitani S, Gengyo-Ando K, Kohara Y. Development. 2003; 130:2495–2503. [PubMed: 12702662]
40. Lai WS, Carballo E, Thorn JM, Kennington EA, Blackshear PJ. J. Biol. Chem. 2000; 275:17827–17837. [PubMed: 10751406]
41. Hudson BP, Martinez-Yamout MA, Dyson HJ, Wright PE. Nat. Struct. Mol. Biol. 2004; 11:257–264. [PubMed: 14981510]
42. Chekulaeva M, Hentze MW, Ephrussi A. Cell. 2006; 124:521–533. [PubMed: 16469699]
43. Wickens M, Goldstrohm A. Science. 2003; 300:753–755. [PubMed: 12730589]
44. Keene JD, Tenenbaum SA. Mol. Cell. 2002; 9:1161–1167. [PubMed: 12086614]

Europe PMC Funders Author Manuscripts

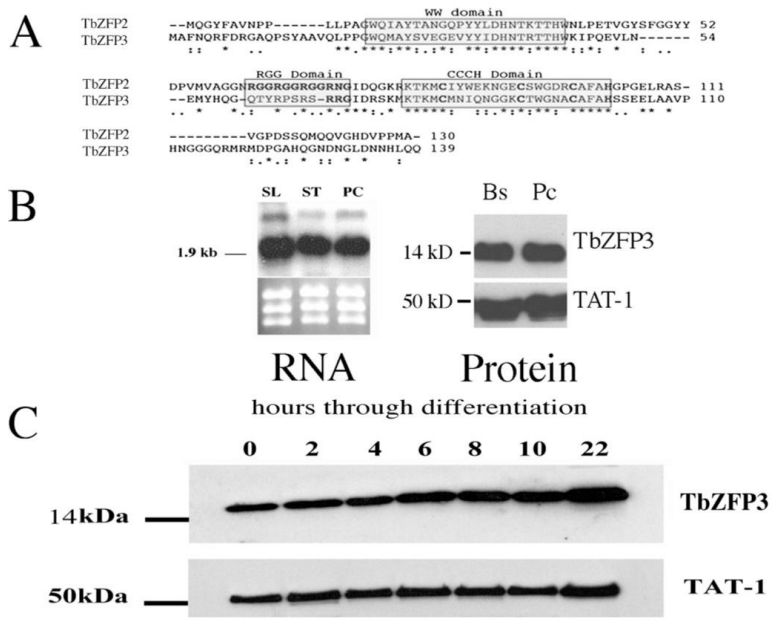

FIGURE 1. Identification and expression of a novel CCCH protein

A, sequence alignment of *Tb*ZFP3 with *Tb*ZFP2, a previously identified small CCCH protein in trypanosomes. The WW, RGG, and CCCH domains are *boxed* in each case, highlighting the similarity in structural organization of the two sequences, despite their lacking obvious primary sequence identity. *B*, expression profile of *Tb*ZFP3 during the trypanosome life cycle. The *left-hand panel* shows a Northern blot of RNA derived from bloodstream slender (*SL*), bloodstream stumpy (*ST*), and procyclic (*PC*) forms hybridized with a *TbZFP3* mRNA-specific Riboprobe. The transcript migrates at 1.9 kb, considerably larger than the coding region of *TbZFP3*, suggesting the presence of untranslated regions extending for ~1.5 kb. The *right-hand panel* shows protein expression of *Tb*ZFP3 in monomorphic bloodstream forms (*Bs*) or procyclic (*Pc*) forms. The protein migrates at the expected molecular mass (14 kDa). Staining with an antibody to trypanosome α-tubulin (*TAT1*) provides a control for loading. *C, Tb*ZFP3 protein expression during synchronous differentiation between a uniform population of bloodstream stumpy forms and procyclic forms. Protein samples were prepared at 2-h intervals during differentiation to procyclic forms. *Tb*ZFP3 expression was relatively uniform during the differentiation time course, matching the expression of α-tubulin, which is detected with the antibody TAT1.

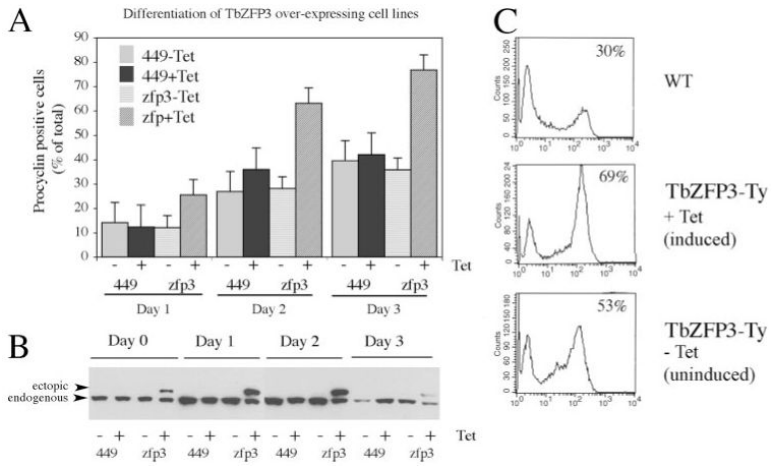

FIGURE 2. TbZFP3 ectopic expression generates an enhanced differentiation phenotype

A, a graph shows the percent EP procyclin expressers in either parental cells in the presence or absence of tetracycline, or in a cell line in which *Tb*ZFP3-Ty expression is inducible. Procyclin expression was monitored for 3 days after exposure of the cells to 6 mM *cis*-aconitate by immunofluorescence. The data represent means of four independent experiments, with the standard error of the mean being presented for each *bar*. *B*, during the differentiation experiments shown in *A*, the expression of endogenous and ectopic *Tb*ZFP3 was monitored using the antibody to *Tb*ZFP3. In each case *Tb*ZFP-Ty expression was detected only in the induced population. *C*, an analysis of EP procyclin expression by flow cytometry. Cells were processed for staining with antibody to EP procyclin at 48 h after the initiation of differentiation, and then the proportion of cells expressing this surface marker was assayed by fluorescence-activated cell sorting. Expression of *Tb*ZFP3-Ty enhances the proportion of cells expressing EP procyclin.

Europe PMC Funders Author Manuscripts

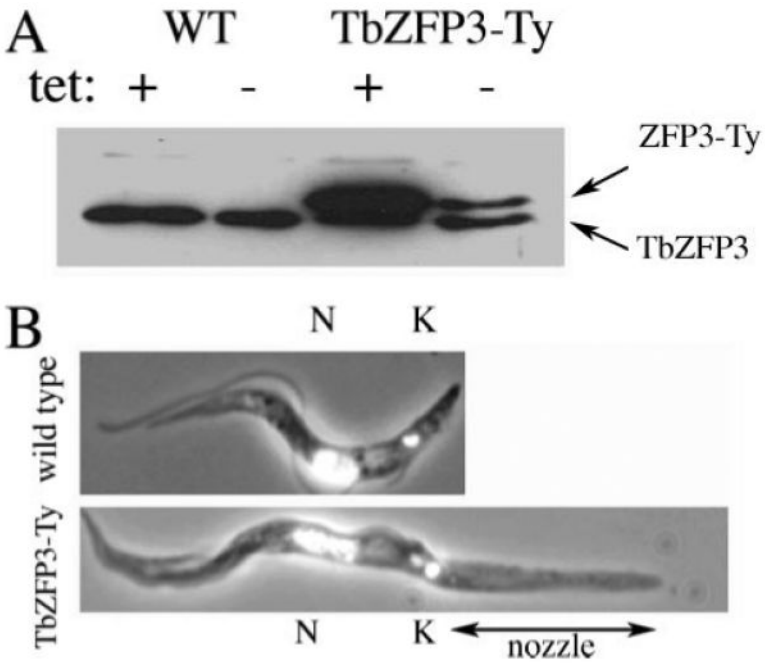

FIGURE 3. Ectopic expression of *Tb*ZFP3-Ty in procyclic forms

A, shows cells in which *Tb*ZFP3-Ty expression is induced (or not) by the presence of tetracycline, together with wild-type controls. In each case *Tb*ZFP3 is detected with the *Tb*ZFP3-specific antibody; ectopic expression of *Tb*ZFP3-Ty is highly expressed in the induced cell population, and also present more weakly in the uninduced cell line (due to incomplete repression). *B*, shows either a wild-type cell, or a cell that has undergone morphological extension at its posterior end following induction of the expression of *Tb*ZFP3-Ty. Note that cell dimensions are unchanged, excepting in the distance between the kinetoplast and cell posterior. *N* = nucleus, *K* = kinetoplast.

Europe PMC Funders Author Manuscripts

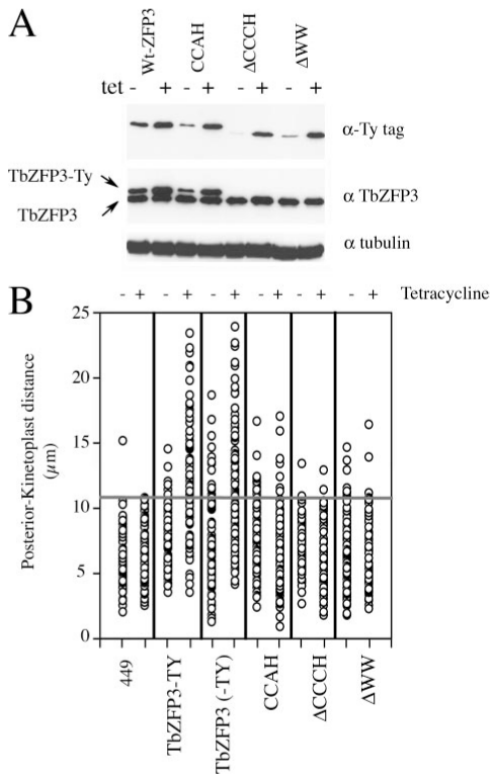

FIGURE 4. Nozzle formation as a phenotypic assay for important domains in TbZFP3

A, ectopic expression of either *Tb*ZFP3-Ty, or mutant derivatives of this in which the WW domain is deleted, the CCCH domain is deleted, or in which the third cysteine in the CCCH domain is mutated to alanine. In each case, expression of the ectopic proteins is detected with the anti-Ty tag antibody, BB2 (*α Ty tag*). Also shown are the same samples hybridized with the *Tb*ZFP3-specific anti-peptide antibody, which detects both the transgenic protein and endogenous *Tb*ZFP3. Note that deletion of the WW or CCCH domains causes the transgenic and endogenous *Tb*ZFP3 to co-migrate. In each case equivalent protein loading is indicated by staining for trypanosome *α*-tubulin. *B*, the kinetoplast-posterior dimension for each cell line either when induced, or not, by the presence of tetracycline. In each case 100 cells were scored, with a *horizontal line* being placed at the position of the longest kinetoplast-posterior dimension in the parental population (*449*) to assist visualization of the appearance of the nozzle phenotype. One cell in the parental population also showed an unusually long kinetoplast-posterior dimension: this is seen very occasionally in such populations but is at a frequency far lower than manifestation of the nozzle phenotype.

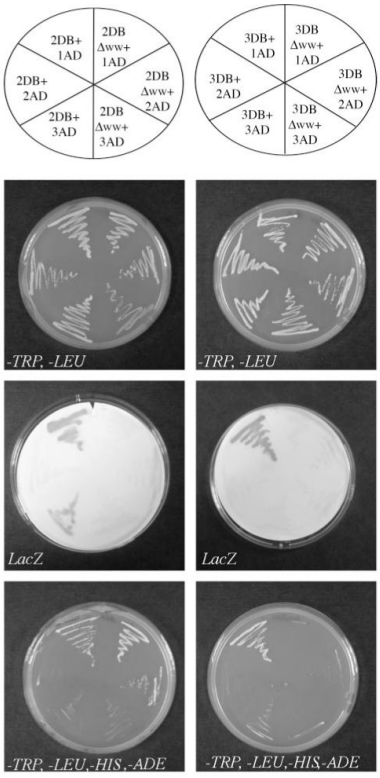

FIGURE 5. Interactions among the TbZFP family assessed by yeast two-hybrid analysis

In each case interactions between intact *Tb*ZFP2 or -3 (*2DB* and *3DB*) or mutant derivatives of these lacking the WW domain (*2DB* Δ *WW* and *3DB* Δ *WW*) fused to the LexA DNA binding domain are shown in combination with *Tb*ZFP1, -2, or -3 fused to the Gal4 activation domain (*1AD, 2AD*, and *3AD*). *Tb*ZFP1-LexA DNA binding domain constructs are not included in this analysis, because they autoactivate. *Tb*ZFP2 and *Tb*ZFP3 LexA DNA binding domain constructs show no autoactivation (not shown).

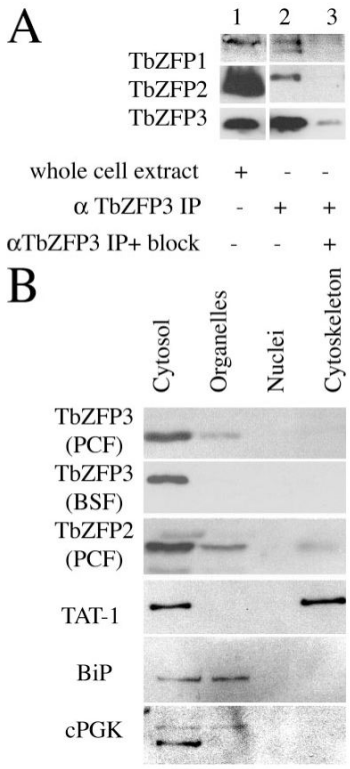

FIGURE 6. Protein interactions and cellular distribution of TbZFP3

A, co-immunoprecipitation of *Tb*ZFP1, -2, and -3 using anti-*Tb*ZFP3 antibody. In each case procyclic cell extracts were subject to immunoprecipitation using anti-ZFP3 antibody and protein G beads. *Tb*ZFP1, -2, and -3 were each immunoprecipitated by *Tb*ZFP3-antibody, the specificity of this interaction being confirmed by inclusion, as a block, of the peptide immunogen against which the antibody was raised. Consistent with earlier results (16) *Tb*ZFP1 signal is detected as a doublet, the relative intensity of which differs between experiments for unknown reasons. *B*, distribution of *Tb*ZFP3 in *T. brucei* bloodstream (*BSF*) or procyclic form (*PCF*) extracts. *Tb*ZFP3 associates with the cytosolic fraction, as does *Tb*ZFP2. Analysis of the same extracts with antibodies for alpha tubulin (cytoskeletal and cytosolic), BiP (endoplasmic reticulum-associated, but with leakage into the cytosol upon cell fractionation), cytosolic phosphoglycerate kinase (cytosolic) confirmed the identity of each fraction. No protein associated with the nuclear fraction.

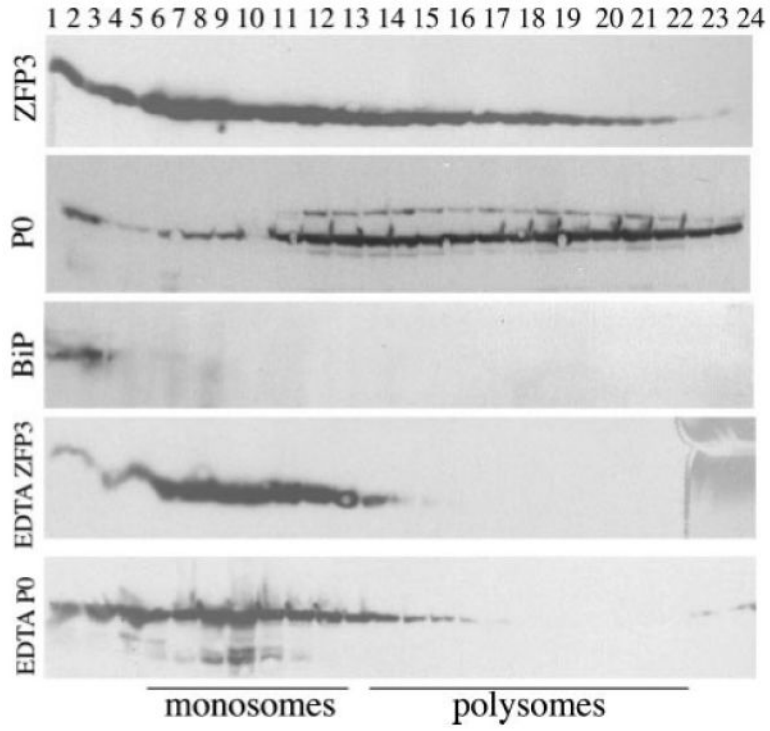

FIGURE 7. TbZFP3 is polysome-associated in procyclic forms

Procyclic form cell extracts were separated on 15-50% sucrose gradients, and the presence of *Tb*ZFP3, the ribosomal protein P0, and the non-ribosomal endoplasmic reticulum protein BiP were detected via specific antibodies against each protein. Lower molecular weight fractions are to the *left* of each profile, high molecular weight polysomal fractions are to the *right*. Extracts were prepared in the presence of cycloheximide or in the presence of EDTA, which disassociates polysomes causing redistribution of *Tb*ZFP3 and P0 into lower molecular weight fractions.

Europe PMC Funders Author Manuscripts

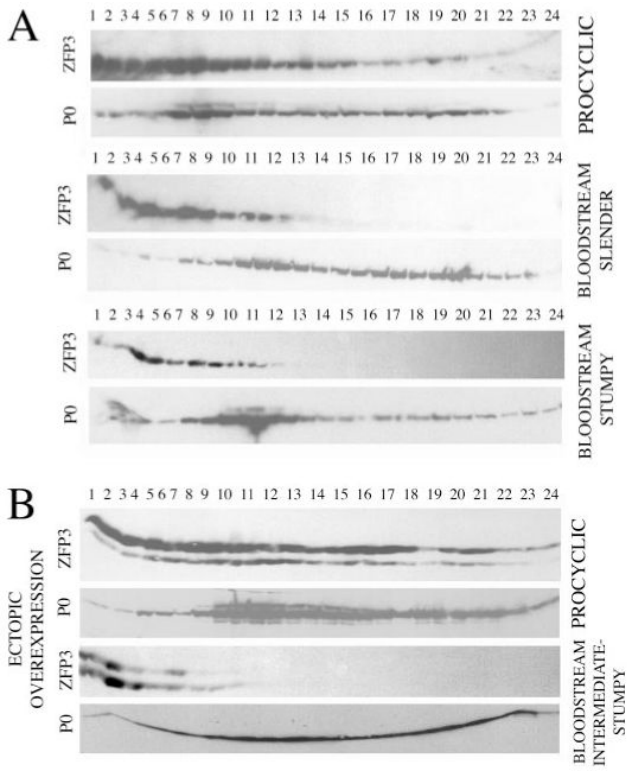

FIGURE 8. Stage-specific polysome association of TbZFP3

A, polysome association of TbZFP3 is procyclic-enriched. The distribution of TbZFP3 or the ribosomal protein P0 is shown in either procyclic forms, bloodstream slender forms, or bloodstream stumpy forms. *B*, ectopic expression of TbZFP3 in procyclic and bloodstream forms. In each case the ectopic protein (which runs slightly larger than the endogenous protein due to the incorporation of a C-terminal Ty epitope tag) co-sediments with the endogenous protein, this being polysomal in procyclic forms, and non-polysomal in bloodstream forms.

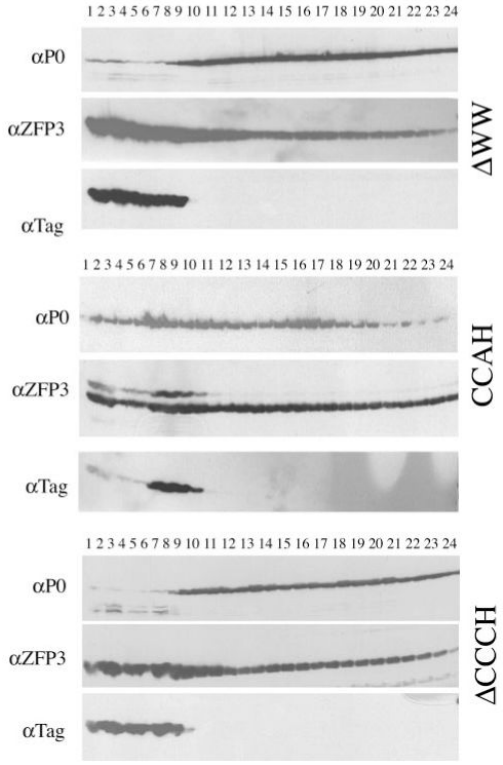

FIGURE 9. Polysomal association of TbZFP3 mutants

Ectopic expression of either *Tb*ZFP-ΔWW, *Tb*ZFP3-CCAH, or *Tb*ZFP3-ΔCCCH was induced in procyclic forms, and the distribution of endogenous and ectopic *Tb*ZFP3 was detected using the *Tb*ZFP3-specific antibody (*α*-*Tb*ZFP3). Specific detection of the ectopic protein was via antibody to the Ty1-eptiope tag incorporated into each mutant protein (*α*-Ty1). The polysomal distribution was determined by antibody to the P0 protein (*α*-P0). Note that the ΔCCCH and ΔWW mutants co-migrate with endogenous TbZFP3, whereas the CCAH mutant runs slightly larger than endogenous TbZFP2 (due to incorporation of the Ty1 epitope tag).

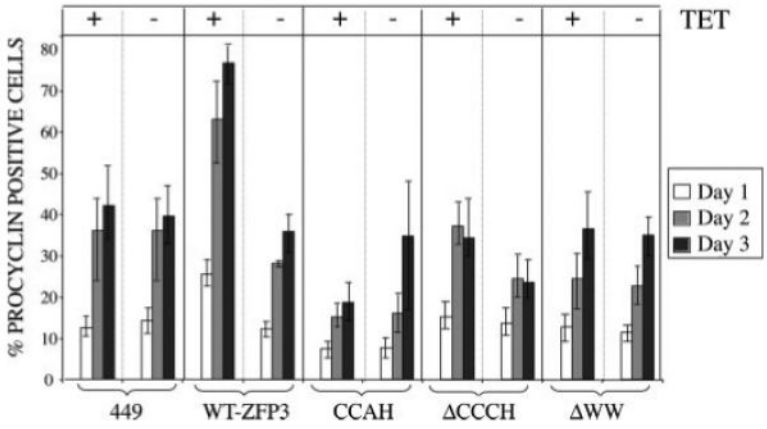

FIGURE 10. Differentiation capacity of bloodstream forms expressing mutant TbZFP3

Differentiation efficiency of transgenic bloodstream lines expressing under tetracycline regulation either intact *Tb*ZFP3 or mutants disrupted for the CCCH domain (CCAH or ΔCCCH) or WW domain. The expression of EP procyclin was scored by immunofluorescence after 24, 48, or 72 h. Data represent the mean of four independent experiments, with *error bars* demonstrating the standard error.

Europe PMC Funders Author Manuscripts

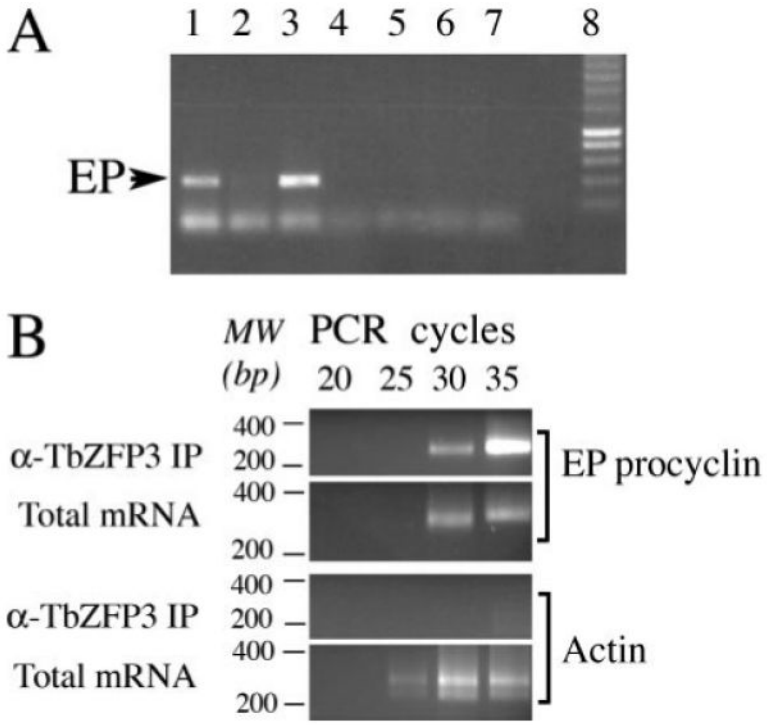

FIGURE 11. Immunoprecipitation of EP procyclin transcripts with TbZFP3

A, EP procyclin mRNA is selected by immunoprecipitation of TbZFP3. *Lane 1*, EP procyclin cDNA amplification after immunoprecipitation with TbZFP3-specific antibody; *lane 2*, as *lane 1*, but with immunoprecipitation being blocked by the *Tb*ZFP3 peptide immunogen; *lane 3*, EP procyclin cDNA amplified from reverse transcribed procyclic form total RNA; *lane 4*, as *lane 3* but without reverse transcriptase; *lane 5*, as *lane 3* but without inclusion of procyclic form mRNA; *lane 6, T. brucei* genomic DNA in place of procyclic form total RNA; *lane 7*, water in place of procyclic form mRNA; *lane 8*, marker. *B*, immunoprecipitation of TbZFP3 differentially selects EP procyclin mRNA with respect to a constitutively expressed transcript. cDNA was derived after RNA immunoprecipitation with anti-TbZFP3 antibody, or derived from unselected total RNA. In each case, an equivalent amount of cDNA was amplified with primers specific for EP procyclin or the constitutively expressed transcript actin in combination with an oligo(dT) anchor, to amplify the 3′-end of each transcript. All amplification reactions were carried out simultaneously with the same source material being used for each. Reaction products were with-drawn every 5 cycles for 35 cycles. EP procyclin mRNA was selected in the immunoprecipitation, whereas actin mRNA was not. In total RNA both transcripts were amplified, with actin mRNA being detected before EP procyclin.